J Solid State Electrochem (2016) 20:1391–1396
DOI 10.1007/s10008-016-3141-7

ORIGINAL PAPER

Composite MWCNT/carbon xerogel-nafion electrode for energy storage

A. S. Ordeñana-Martínez[1] · **M. E. Rincón**[2]

Received: 2 December 2015 / Revised: 10 January 2016 / Accepted: 25 January 2016 / Published online: 5 February 2016

Abstract In this paper, we report the preparation and characterization (morphological, structural, surface, and electrochemical) of multiwalled carbon nanotube (MWCNT)/carbon xerogel (CX) electrodes prepared by mixing. This research proposes the hypothesis that the use of a hydrophilic binder (nafion) and the use of MWCNTs enhance electrode capacitance and conductivity. Electrochemical measurements in 2 M NaCl solution were performed. The advantage of adding multiwalled carbon nanotubes to the array of xerogel-nafion was studied through different electrochemical methods. It was validated that the greater carbon nanotube mesoporosity allows less compaction of the electrode, thus effectively increasing the specific area and therefore capacitance. Furthermore, we observed the increase in electronic conductivity reported in numerous studies, a fact that is true for *iR* drop measurement cycles in both galvanostatic charging and discharging. The carbon composite proved to be viable for energy storage.

Keywords Composite · Carbon nanotubes · Carbon xerogel · Nafion

✉ A. S. Ordeñana-Martínez
alfredosilverio.ordenana@upaep.mx

[1] Decanato de Ciencias Biológicas, Maestría Ingeniería Ambiental y Desarrollo Sustentable, Universidad Popular Autónoma del Estado de Puebla UPAEP, 21 Sur 1103, CP 72410 Puebla, Puebla, Mexico

[2] Instituto de Energías Renovables, Universidad Nacional Autónoma de México, Apartado Postal 34, 62580 Temixco, Morelos, Mexico

Introduction

Carbon aerogels, cryogels, and xerogels have been extensively studied as nanostructured electrode supports for energy storage and conversion applications [1–4]. The most widely used preparation method involves carbon xerogel pulverization; powder is subsequently mixed with binders in order to promote adherence and enable fabrication of film electrodes. A more recent work has reported carbon xerogels on porous materials (carbon cloth) or in the form of monoliths [5, 6]. The advantages of the more recent preparation methods are the absence of binders that would limit the electrical conductivity of the porous electrode and better electric transport on the nanocarbon surface (covalence between particles ensures percolation). In this investigation, we obtained carbon xerogel monoliths of high hardness; however, a great deal of material was lost when the carbon xerogel was sliced with a diamond saw. Thus, we decided to pulverize the carbon xerogel. The development of new materials with very high specific surface areas and the use of porous carbon with different morphologies and different electrical conductivity introduce new possibilities in electrode materials for electrochemical capacitors [7–12]. The weight ratio of multiwalled carbon nanotube (MWCNT)/porous carbons varies in each research [4, 12, 13]. Higher electrical conductivity is always desired to have high capacitance and high power density in super capacitors [14]. This is the main reason to introduce MWCNTs in carbon xerogel [4, 12]. On the other hand, interesting properties are given by the presence of MWCNTs which exhibit a developed porosity, a high electrical conductivity, and a good resilience, all being very important for enhancing the power and cycle life of supercapacitors [4]. This study

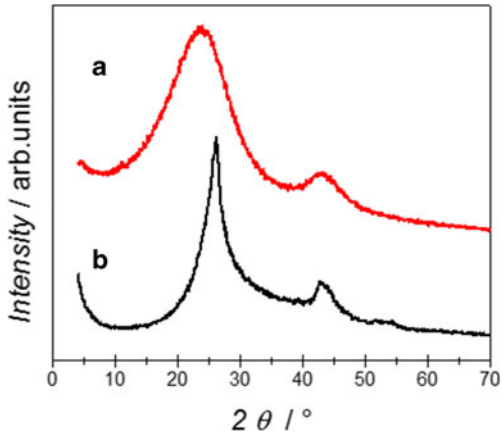

Fig. 1 XRD patterns; (*a*) MWCNT and (*b*) carbon xerogel

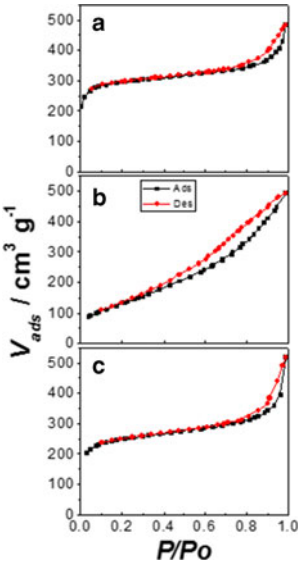

Fig. 2 N_2 adsorption-desorption isotherms; (**a**) CX, (**b**) MWCNT, and (**c**) composite MWCNT:CX (10:90)

proposes that the employment of a hydrophilic binder (nafion) and the incorporation of MWCNTs would improve the capacitance and conductivity of the composite. The electrodes were prepared by mixing and the electrochemical characterization was carried out in 2 M NaCl solution.

Material and methods

The synthesis procedure for the carbon xerogels was similar to that reported elsewhere [1]. Resorcinol-formaldehyde (RF) gels were prepared by the reported polycondensation of resorcinol (R) (99 %, Sigma-Aldrich) and formaldehyde (F) (37 wt%, Sigma-Aldrich), using Na_2CO_3 (J.T. Baker) as the catalyst (C), at fixed molar ratios of R:F (1:2) and R:C (1000:1). After gelation at 50 °C for 96 h, the gels were dried at ambient conditions for 72 h, followed by an acetone bath at 56 °C for 96 h. Carbon xerogels (CX) were obtained by slowly heating (2 °C min^{-1}) the RF gels in nitrogen up to 800 °C for 1 h. To decrease the hydrophobic nature of the xerogels, oxygen-containing functional groups were grafted on the carbon surface through thermal activation in air at 450 °C for 2 h. Multiwalled carbon nanotubes (MWCNTs) purchased from Nanostructured and Amorphous Material Inc. (90 % purity, O.D. <10 nm L ~ 5–15 μm) were subjected to acid treatment [15]. Carbon xerogel-nafion (CXN) films were prepared by mixing 0.166 mg of the thermally activated carbon xerogels with 4.93 μL Nafion solution (Nafion® perfluorinated resin solution 5 wt% in lower aliphatic alcohols and water contains 15–20 % water, Sigma-Aldrich) and spraying over stainless steel substrates. Composite MWCNT/carbon xerogel-nafion (CXMWN) electrode films were prepared in the same way: 0.166 mg of carbon (MWCNT/CX: 10/90 weight ratio) with 4.93 μL Nafion solution and spraying over stainless steel substrates.

Table 1 Temperature and degassing time

Nanocarbon	*T* (°C)	*t* (h)
Carbon xerogel	200	2
MWCNT	200	16

The starting carbon nanomaterials were analyzed by X-ray diffraction (XRD) using a Rigaku® Dmax 2200 diffractometer, with CuKα radiation (λ = 0.154 nm); the crystallite size was calculated by means of the Debye-Scherrer equation [16]:

$$D = \frac{K\lambda}{\beta\cos\theta} \quad (1)$$

where K = 0.9, β (in radians) is the diffraction peak width at medium height, and θ is the diffraction angle.

Nitrogen adsorption and desorption isotherms were measured at 77 K using a Quantacrhome® NOVA 2400 surface area analyzer. The specific surface areas (SBET) of all the carbons and the mixture of carbons (MWCNT/CX: 10/90 weight ratio) were calculated by the Brunauer-Emmett-Teller (BET) method using adsorption data in the relative pressure range of 0.01 to 0.30. The total pore volume was estimated to be the liquid volume of nitrogen at a relative pressure of around 0.99 (V_{pore}). The micropore volume (V_{micro}) was calculated using the *t*-plot (de Boer method). The mesopore volume (V_{meso}) was determined by subtracting the micropore volume from the total volume. The micropore surface area (S_{micro}) and external surface (S_{meso}) were calculated using the *t*-plot (de Boer method) [17]. Pore size distribution was obtained from the nitrogen

Table 2 Specific surface area and pore characteristics of carbons and composite

Nanocarbon	S_{BET} ($m^2\ g^{-1}$)	S_{meso} ($m^2\ g^{-1}$)	S_{micro} ($m^2\ g^{-1}$)	V_{poro} ($cm^3\ g^{-1}$)	V_{meso} ($cm^3\ g^{-1}$)	V_{micro} ($cm^3\ g^{-1}$)	*DFT* (nm)
CX	985	354	631	0.83	0.51	0.32	1.50
MWCNT	495	495	0	0.76	0.76	0	2.80
MWCNT:CX (10:90)	792	305	487	0.80	0.55	0.25	1.50

Table 3 S_{meso}/S_{micro} and V_{meso}/V_{micro} relationship of carbon xerogel and MWCNT/carbon xerogel

Nanocarbon	S_{meso}/S_{micro}	% S_{meso}	% S_{micro}	V_{meso}/V_{micro}	% V_{meso}	% V_{micro}
CX	0.56	36	64	1.6	62	39
MWCNT: CX (10:90)	0.63	39	62	2.2	69	31

adsorption data based on density functional theory (DFT) [18].

Electrochemical measurements were carried out using a three-electrode cell using graphite as counter electrode and SCE as reference electrode. A Metrohm® Autolab PGSTAT302N was used for cyclic voltammetry and galvanostatic charge/discharge measurements. Analysis of the electrode surface was performed with a scanning electron microscope (Hitachi® FE-SEM, S-5500) working at 5–6 kV of operating voltage.

Results and discussion

Figure 1 compares the XRD patterns of the functionalized MWCNTs and the thermally activated carbon xerogel (two peaks at $2\theta = 25°$ and $2\theta = 45°$). The broad peaks were fitted with Lorentzian peaks for a reliable estimation of crystallite size. For the MWCNTs (Fig. 1a), the estimated crystallite size of 1.8 nm (~6 graphene layers) was within the range given by the manufacturer, but it suggests a relatively large inner diameter or a broad distribution of outer/inner pore diameters in commercial nanotubes. Concerning carbon xerogel (Fig. 1b), we obtained a low value of 0.4 nm, which indicates the abundance of turbostratic or amorphous carbon.

Sample degassing is very important when studying surface area and pore size. As a consequence, degassing time and temperature must be optimized in order to avoid high temperatures or long degassing times causing irreversible damage to samples, which could in turn result in a decrease of specific area due to the sintering process, or an increase in specific area due to thermal decomposition of the sample. Whereas the degassing time for MWCNTs is standardized, carbon xerogel degassing time is not, so different tests were performed. Table 1 shows temperature and degassing time for the carbons.

The nitrogen adsorption-desorption isotherms of carbons and composite MWCNT:carbon xerogel (10:90) are shown in Fig. 2. It can be appreciated that the adsorption isotherms of all carbons are type IV (IUPAC), type H4 hysteresis loops (IUPAC) to carbon xerogel and composite (Fig. 2a, c), and type H3 hysteresis loop to MWCNT (Fig. 2c). These indicate that there is a higher amount of micropores in xerogel carbon and greater mesoporosity in functionalized nanotubes, while

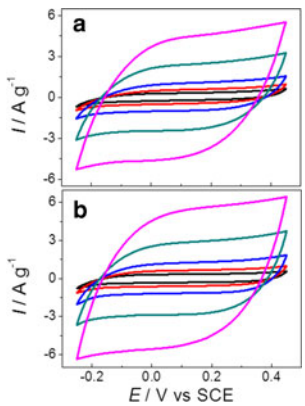

Fig. 3 Cyclic voltammograms in 2 M NaCl at 5 (black line), 10 (red), 20 (blue), 50 (green) and 100 mV s^{-1} (pink) ; **a** CX and **b** CXMWN

Table 4 CX and CXMWN capacitances at different scan rates

Electrode	ν (mV s^{-1})	C_{charge} (F g^{-1})	$C_{discharge}$ (F g^{-1})
CXN	5	51	61
	10	50	55
	20	49	51
	50	48	48
	100	44	44
CXMWN	5	63	67
	10	60	64
	20	58	62
	50	57	57
	100	53	54

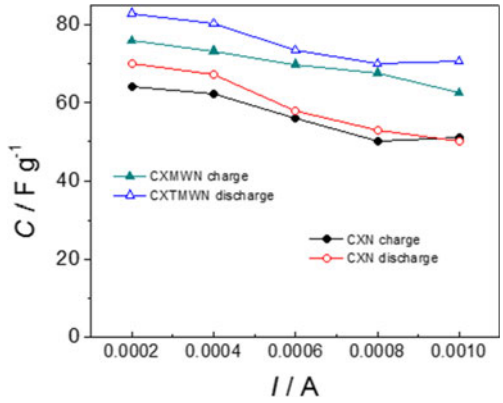

Fig. 4 A variation of capacitance determined from galvanostatic charge/discharge cycles in 2 M NaCl

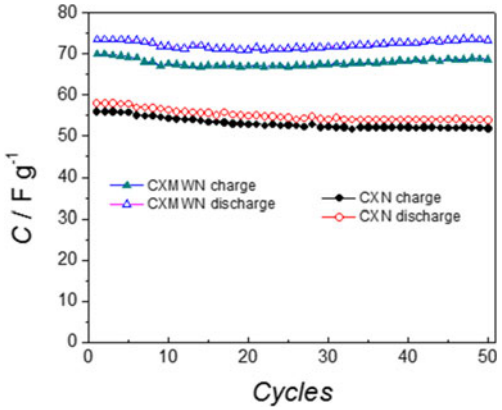

Fig. 5 Specific capacitance versus charge/discharge cycles; CXN and CXMWN at $I = 6 \times 10^{-4}$ A in 2 M NaCl

the composite presents an intermediate behavior, although closest to xerogel carbon. According to the hysteresis loops (H3 and H4), the pores are of the slit-shaped kind.

The textural characteristics of these carbons are summarized in Table 2. Analysis of the results leads to the conclusion that there are no micropores in MWCNTs, while 64 % of the carbon xerogel BET area corresponds to micropores and 36 % to mesopores (in regard to pore volume, 61.5 % corresponds to mesopores and 38.5 % to micropores). As is shown in the Table 3, the added 10 % weight of the MWCNTs to carbon xerogel enhances the S_{meso}/S_{micro} and V_{meso}/V_{micro} relationship, which could be beneficial for the energy storage performance of these materials (greater penetration of the solvated ions).

Figure 3 compares the cyclic voltammetry curves (1-cm^2 electrodes) in the range of −0.25 to 0.45 V versus SCE at speeds of 5, 10, 20, 50, and 100 mV s^{-1} in 2 M NaCl. The values of specific current are normalized in regard to carbon xerogel mass. In general, we can see that the experiments performed at different scan rates show an increase in current as the scan rate is increased without any significant degeneration in the form of voltammograms at a high scan rate. Differences between carbon xerogel-nafion (CXN) and carbon nanotubes/carbon xerogel-nafion (CXMWN) are difficult to determine, but it appears that the addition of carbon nanotubes improves the shape of the curve at high scan rates due to less resistance (see Table 4). It can be seen that capacitances obtained with CXMWN are higher than those of CXN, e.g., 62 versus 51 F g^{-1} at 20 mV s^{-1} in discharge.

Chronopotentiometry determined charge/discharge performance by setting a specific current. To this end, a double pulse of current was applied to CXN and CXMWN for 50 cycles. The magnitude of the current was selected considering the voltammetric response of the electrodes. For carbons in 2 M NaCl, the demanded currents were $\pm 2 \times 10^{-4}$ A, $\pm 4 \times 10^{-4}$ A, $\pm 6 \times 10^{-4}$ A, $\pm 8 \times 10^{-4}$ A, and $\pm 10 \times 10^{-4}$ A. The specific capacitance as a function of the applied current is shown in Fig. 4. The values of CXN and CXMWN electrodes' specific capacitance obtained from galvanostatic charge/discharge measurements are given in Table 5.

Figure 5 shows specific capacitance compared to charge/discharge cycles of the CXN and CXMWN electrodes at $I = 6 \times 10^{-4}$ A (which corresponds to that obtained in the cyclic voltammetry measurements carried out at 20 mV s^{-1}). Good stability could be appreciated during the first 50 cycles. In fact, the CXMWN electrode presents a slight increase in specific capacitance during the last galvanostatic cycles. It can be seen too that capacitances obtained with CXMWN are higher than those of CXN, e.g., 73 versus 58 F g^{-1} at $I = 6 \times 10^{-4}$ A in discharge. The specific capacitance and good stability of the CXMWN are better due to the presence of

Table 5 CXN and CXMWN capacitance determined from galvanostatic charge/discharge in 2 M NaCl

	CXN		CXMWN	
I (A)	C_{charge} (F g^{-1})	$C_{discharge}$ (F g^{-1})	C_{charge} (F g^{-1})	$C_{discharge}$ (F g^{-1})
$\pm 2 \times 10^{-4}$	66	69	75	82
$\pm 4 \times 10^{-4}$	62	67	73	80
$\pm 6 \times 10^{-4}$	**56**	**58**	**70**	**73**
$\pm 8 \times 10^{-4}$	50	53	68	70
$\pm 10 \times 10^{-4}$	51	50	63	71

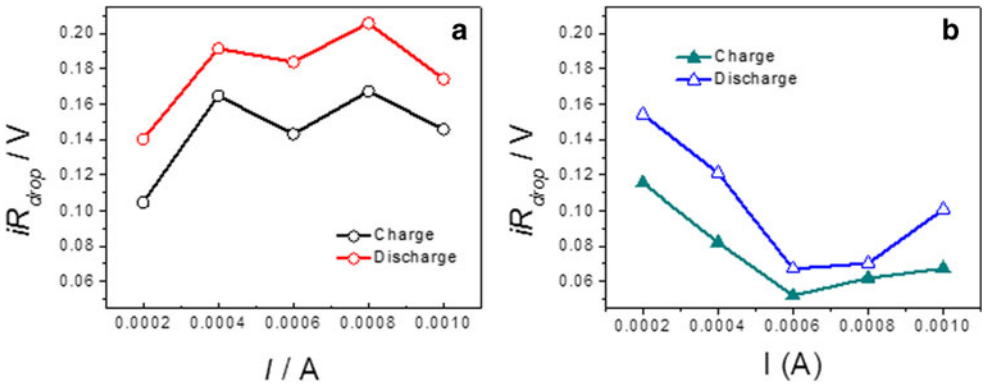

Fig. 6 Drop *iR* **a** CXN and **b** CXMWN at different electric currents

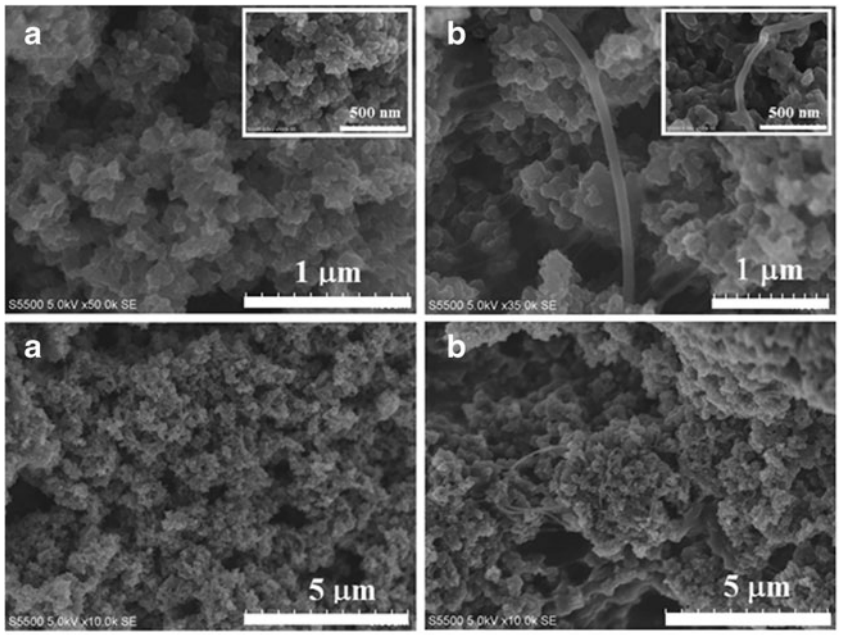

Fig. 7 SEM images of electrodes: **a** CXN and **b** CXMWN. Insets: magnification 100,000 (500 nm) **a** CXN and **b** CXMWN

MWCNTs, which increase the mesoporosity and the electronic conductivity of composite.

The *iR* drop value for the CXN and CXMWN electrodes was determined. Figure 6 shows the behavior observed in the charge/discharge stages for both electrodes. The lowest *iR* drop occurred in the CXMWN matrix; this is attributed to the incorporation of MWCNTs, which provide electronic conductivity and mesoporosity to the electrode. This lower *iR* drop improved the electrode capacitance. It was also noted that the *iR* drop decreases as the electric current increases, which means that MWCNTs play a role in the reduction of resistance (mesoporosity and high electrical conductivity). The opposite occurs with the CXN electrode, which becomes more resistive with increasing current.

SEM images (Fig. 7 and Fig. 8) were obtained in order to elucidate the causes of CXMWN composites' higher conductivity. The image shows that porosity is similar for both (or even better for CXMWN). Moreover, it is observed that MWCNTs are incorporated throughout the bulk of the carbon xerogel-nafion matrix. The incorporation of 10 % by weight of carbon nanotubes seems to be at the percolation limit, which explains the electronic conductivity increase.

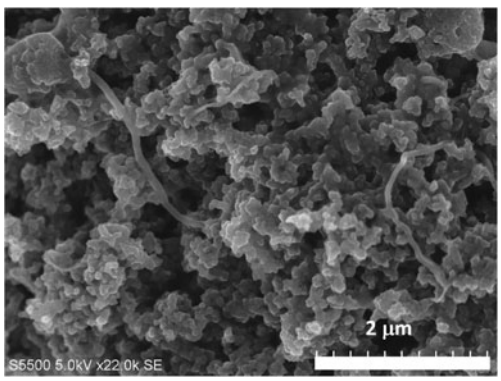

Fig. 8 SEM image of CXMWN

Conclusions

This study reports the preparation and electrochemical characterization of CXN and CXMWN electrodes by the mixing method. The addition of MWCNTs enhances the capacitance and mechanical properties of the composite. Nafion was selected as the most suitable binder for the preparation of electrode films owing to its good performance over a wide range of scan rates. It was validated that the greater mesoporosity of the carbon nanotube allows reduced compaction of the electrode, thereby increasing the effective area and thus capacitance. Furthermore, the increase in electronic conductivity reported in many papers was observed, which was validated by measuring the *iR* drop in the galvanostatic charge/discharge. The composite CXMWN is proposed as an electrode for studies on energy storage.

Acknowledgments We thank G. Hernández-Cruz and R. Morán for the technical assistance, and the financial support from projects of CONACYT.

References

1. Ordeñana-Martínez AS, Rincón ME, Vargas M, Estrada-Vargas A, Casillas N, Bárcena-Soto M, Ramos E (2012) Carbon nanotubes/carbon xerogel-nafion electrodes: a comparative study of preparation methods. J Solid State Electrochem 16:3777–3782
2. Calvo EG, Lufrano F, Arenillas A, Brigandì A, Menéndez JA, Staiti P (2014) Effect of unequal load of carbon xerogel in electrodes on the electrochemical performance of asymmetric supercapacitors. J Appl Electrochem 44:481–489
3. Inagaki M, Kang F, Toyoda M, Konno H (2014) Chapter 11—carbon materials for electrochemical capacitors. Advanced materials science and engineering of carbon 237–265
4. Fernández PS, Castro EB, Real SG, Visintin A, Arenillas A, Calvo EG, Juárez-Pérez EJ, Menéndez AJ, Martins ME (2012) Electrochemical behavior and capacitance properties of carbon xerogel/multiwalled carbon nanotubes composites. J Solid State Electrochem 16:1067–1076
5. Wang J, Glora M, Petricevic R, Saliger R, Proebstle H, Fricke J (2001) Carbon cloth reinforced carbon aerogel films derived from resorcinol formaldehyde. J Porous Mater 8:159–165
6. Villar I, Suarez-De la Calle DJ, González Z, Granda M, Blanco C, Menéndez R, Santamaría R (2011) Carbon materials as electrodes for electrosorption of NaCl in aqueous solutions. Adsorption 17:467–471
7. Béguin F (2006) Application of nanotextured carbons for electrochemical energy storage in aqueous medium. J Braz ChemSoc 17:1083–1089
8. Simon P, Gogotsi Y (2008) Materials for electrochemical capacitors. Nat Mater 7:845–854
9. Niu C, Sichel EK, Hoch R, Moy D, Tennent H (1997) High power electrochemical capacitors based on carbon nanotube electrodes. Appl Phys Lett 70:1480–1482
10. Jurewicz K, Vix-Guterl C, Frackowiak E, Saadallah S, Reda M, Parmentier J, Patarin J, Béguin F (2004) Capacitance properties of ordered porous carbon materials prepared by a templating procedure. J Phys Chem Solids 65:287–293
11. Cebeci FÇ, Sezer E, Sarac AS (2009) A novel EDOT–nonylbithiazole–EDOT based comonomer as an active electrode material for supercapacitor applications. Electrochim Acta 54:6354–6360
12. Alia AA, Eltabeyb MM, Abdelbaryc BM, Zoalfakar SH (2015) MWCNTs/carbon nanofibril composite papers for fuel cell and supercapacitor applications. J Electrost 73:12–18
13. Zhao TK, Liu LH, Li GM, Du L, Zhao X, Yan J, Cheng YL, Dang A, Li TH (2012) Preparation and electrochemical property of CMC/MWCNT composite using ionic liquid as solvent. Letter Materials Science Chinese Science Bulletin 57:1620–1625
14. Dalton AB, Collins S, Muñoz E, Razal JM, Ebron VH, Ferraris JP, Coleman JN, Kim BG, Baughman RH (2003) Super-tough carbon-nanotube fibers. Nature 423:703–703
15. Ordeñana-Martínez AS, Rincón ME, Vargas M, Ramos E (2011) Impedance response of carbon nanotube-titania electrodes dried under modified gravity. Thin Solid Films 519:5403–5407
16. Cullity BD (1978) Elements of X-ray diffraction. Addison-Wesley Publishing Company Inc. Reading, MA, 262
17. Passe-Coutrin N, Altenor S, Cossement D, Jean-Marius C, Gaspard S (2008) Comparison of parameters calculated from the BET and Freundlich isotherms obtained by nitrogen adsorption on activated carbons: a new method for calculating the specific surface area. Microporous Mesoporous Mater 111:517–522
18. Wang A, Kang F, Huang Z, Guo Z, Chuan X (2008) Synthesis of mesoporous carbon nanosheets using tubular halloysite and furfuryl alcohol by a template-like method. Microporous Mesoporous Mater 108:318–324